METABOLIC DISORDERS

Role of Toll-like receptors in diabetic renal lesions in a miniature pig model

Yuanyuan Feng,[1]* Shulin Yang,[2]* Yuxiang Ma,[1] Xue-Yuan Bai,[1]† Xiangmei Chen[1]†

The mechanisms of diabetic renal injury remain unclear. Recent studies have shown that immunological and inflammatory elements play important roles in the initiation and development of diabetic nephropathy (DN). Toll-like receptors (TLRs) comprise a superfamily of innate immune system receptors. The roles and mechanisms of TLRs in the pathogenesis of diabetic renal lesions are mostly unknown. Compared with rodents, miniature pigs are more similar to humans with respect to metabolism, kidney structure, and immune system, and therefore represent an ideal large-animal model for DN mechanistic studies. A diabetes model was established by feeding miniature pigs with high-sugar and high-fat diets. Functional and pathological markers, expression and activation of endogenous TLR ligands [HSP70 (heat shock protein 70) and HMGB1], TLR1 to TLR11 and their downstream signaling pathway molecules (MyD88, IRAK-1, and IRF-3), nuclear factor κB (NF-κB) signaling pathway molecules (IKKβ, IκBα, and NF-κBp65), inflammatory cytokines [IL-6 (interleukin-6), MIP-2, MCP-1, CCL5, and VCAM-1 (vascular cell adhesion molecule–1)], and infiltration of inflammatory cells were systematically evaluated. The expression of HSP70 was significantly increased in diabetic pig kidneys. The expression of MyD88-dependent TLR2, TLR4, TLR5, TLR7, TLR8, and TLR11 and their downstream signaling molecules MyD88 and phospho–IRAK-1 (activated IRAK-1), as well as that of MyD88-independent TLR3 and TLR4 and their downstream signaling molecule phospho–IRF-3 (activated IRF-3), was significantly up-regulated. The expression and activation of NF-κB pathway molecules phospho-IKKβ, phospho-IκBα, NF-κBp65, and phospho-NF-κBp65 were significantly increased. Levels of IL-6, MIP-2, MCP-1, CCL5, VCAM-1, and macrophage marker CD68 were significantly increased in diabetic pig kidneys. These results suggested that the metabolic inflammation activated by TLRs might play an important role in diabetic renal injuries.

INTRODUCTION

In recent years, with the changes in dietary structures and lifestyles, the incidences of diabetes mellitus (DM) and diabetic nephropathy (DN) consequent to excessive nutrient intake have increased every year (1). DN is among the most common complications of DM and a major cause of renal failure. Studies have shown that renal injuries such as glomerular hypertrophy and capillary basement membrane thickening are already occurring in early-stage DM (2). However, the exact mechanisms by which DM causes kidney damage remain unclear and there are no specific prevention and treatment measures. Therefore, clarification of the pathogenic mechanisms of DM-associated renal lesions is important to develop prevention and treatment methods.

Metabolic inflammation differs from traditional pathogenic microbe-induced inflammation; it is a type of low-level, chronic, and atypical inflammation mainly induced by excess nutrient intake (3). Recent studies have shown that metabolic inflammation plays an important role in the tissue and organ damage caused by chronic metabolic diseases (4, 5). Toll-like receptors (TLRs) are important receptors of the innate immune system that act within the body, and exogenous pathogens can bind to TLRs to activate downstream inflammation signal transduction pathways and initiate the adaptive immune response. Recent studies have shown that some endogenous ligands such as heat shock proteins (HSP), extracellular matrix degradation products, S100

protein family members, heparan sulfate, nucleic acids, and sugars and fatty acids at high levels can bind to intracellular and extracellular TLRs to induce inflammation. TLR2 and TLR4 are associated with acute kidney injury, chronic kidney diseases, and the occurrence of DN (6–9). However, a systematic understanding of the role of the entire molecules in the TLR system in DM-induced renal damage remains limited.

In recent years, rodent DM models have been established to study the mechanism of renal injury in DM (10). However, because there are considerable differences between rodents and humans with respect to genetics, anatomy, physiology, and metabolism, studies based on rodents cannot accurately simulate the pathogenic processes of human disease. Humans and mice were found to differ significantly with respect to immune inflammatory systems, including the TLR system and inflammatory responses (11). Compared with rodents, pigs (especially miniature pigs) more closely resemble humans with respect to metabolism, physiology, and pathology, and thus can better simulate the processes of human disease (12, 13). The kidneys of miniature pigs are very similar to those of humans in terms of anatomy, size, shape, and physiological functions (14). For example, there is a multilobular, multipapillary architecture in the kidneys of humans and mini pigs, whereas mice, rats, dogs, and rabbits have unilobular, unipapillary kidneys (15). Among the commonly used large experimental animals, dogs are carnivores and monkeys are herbivores, whereas only pigs are omnivores, similar to humans. In addition, miniature pigs provide greater ethical and economic advantages (16). Therefore, miniature pigs are an ideal animal model to investigate human disorders such as metabolic and kidney diseases.

Here, we established a diabetes model by feeding Chinese Bama mini pigs with high-sugar and high-fat diets and systematically investigated the changes in the TLR system and associated downstream signaling pathways, the nuclear factor κB (NF-κB) signaling pathway, and the

[1]Department of Nephrology, Chinese PLA General Hospital, Chinese PLA Institute of Nephrology, State Key Laboratory of Kidney Diseases, National Clinical Research Center for Kidney Diseases, Beijing 100853, China. [2]Key Laboratory for Farm Animal Genetic Resources and Utilization of Ministry of Agriculture of China, Institute of Animal Science, Chinese Academy of Agricultural Science, Beijing 100193, China.
*These authors contributed equally to this work.
†Corresponding author. E-mail: xueyuan_bai@163.com (X.-Y.B.); xmchen301@126.com (X.C.)

TLR system–mediated inflammation in diabetic renal injuries, to explore the role of TLRs in diabetic renal damage.

RESULTS

Blood biochemical changes in the diabetes model

In Table 1, after miniature pigs in the DM group were fed a high-sugar and high-fat diet for 8 months, the levels of fasting blood glucose (GLU) and insulin (INS) were significantly increased in the DM group compared to those in the CON (normal control) group ($P < 0.05$). The levels of triglyceride (TG), total cholesterol (CHOL), and low-density lipoprotein cholesterol (LDL-C) were also significantly increased ($P < 0.05$)

Table 1. Blood biochemical results in the miniature swine diabetes model. Values are means ± SD. CON, normal control group; DM, diabetes group.

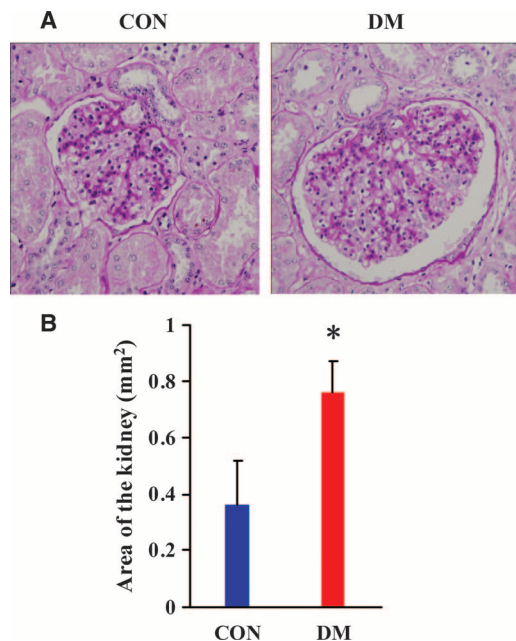| Paramaters	CON	DM
GLU (mM)	5.29 ± 0.91	9.95 ± 0.96*
INS (μIU/ml)	4.97 ± 1.18	23.63 ± 13.2*
TG (mM)	0.29 ± 0.04	0.62 ± 0.08*
CHOL (mM)	1.33 ± 0.14	2.22 ± 0.6*
HDL-C (mM)	0.39 ± 0.06	0.49 ± 0.11
LDL-C (mM)	0.64 ± 0.07	1.12 ± 0.37*
Creatinine (μM)	204.5 ± 15.93	119.42 ± 18.82
BUN (mM)	8.21 ± 1.61	3.72 ± 1.78

*$P < 0.005$ versus CON.

Fig. 1. Kidney PAS staining and glomerular area score results of diabetic miniature pigs. (**A**) PAS staining results of the kidneys of diabetic miniature pigs. (**B**) Score results of glomerular area. CON, normal control group; DM, diabetes group. Magnification, ×400. Glomerular areas are presented as means ± SD. *$P < 0.05$ versus CON.

in the DM group, and the changes in high-density lipoprotein cholesterol (HDL-C) levels were less obvious in the DM group. No significant changes were observed in creatinine and blood urea nitrogen (BUN) levels of plasma between DM and CON mini pigs.

Pathological changes in diabetic kidneys

On the basis of periodic acid–Schiff (PAS) staining, the kidneys in the DM group showed significant pathological changes such as marked glomerular hypertrophy, whereas there were no obvious histological alterations in the kidneys of the CON group (Fig. 1). The statistical results for the glomerular area showed that the glomerular areas in the DM group kidneys were significantly larger than those in the CON group ($P < 0.001$; Fig. 1). This suggested that the miniature pigs fed with high-sugar and high-fat diets showed typical manifestations of early diabetes in the kidney tissues (17).

Expression changes in endogenous TLR ligands in diabetic kidneys

HSP70 and HMGB1 are endogenous ligands of TLRs that can bind TLRs and activate inflammatory responses. We used Western blot to detect the changes in HMGB1 and HSP70 protein expression in the kidneys from both groups of miniature pigs. Low levels of HSP70 and HMGB1 expression were observed in the kidneys from the CON group. In contrast, HSP70 expression was significantly upregulated in the kidneys from the DM group, whereas no significant change was observed in HMGB1 expression (Fig. 2).

Expression changes in MyD88-dependent TLRs in diabetic kidneys

All TLRs (excluding TLR3) can activate the MyD88-dependent signaling pathway after binding with ligands; TLR4 can activate both MyD88-dependent and MyD88-independent signaling pathways. We used Western blot to detect the changes in protein expression of TLR1, TLR2, and TLR4 to TLR11 in the kidneys of both groups of miniature
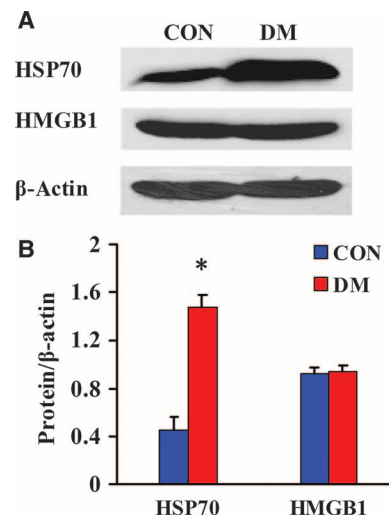

Fig. 2. Expression of TLR endogenous ligand was analyzed by Western blot in the kidney tissues from diabetic miniature pigs. (**A**) Detection of TLR endogenous ligand expression by Western blot. (**B**) Semiquantitative analysis of expression levels of the TLR endogenous ligand. Protein expression data are presented as means ± SD. *$P < 0.05$ versus CON.

pigs. The results showed that the expression levels of TLR2, TLR4, TLR5, TLR7, TLR8, and TLR11 were significantly higher in the DM kidneys than in the CON kidneys, whereas the expression levels of TLR1, TLR6, TLR9, and TLR10 did not change significantly (Fig. 3). We further examined the changes in the expression levels of TLR2 and TLR4 via immunohistochemistry. The results showed that the TLR2 and TLR4 staining intensities were significantly higher in the kidney tissues from DM than those from CON, and these proteins were mainly expressed on renal tubular epithelial cells (Fig. 4).
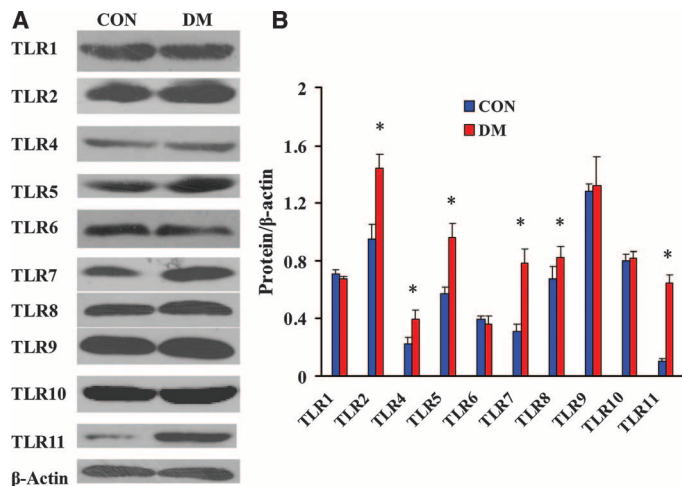

Fig. 3. Western blot analysis of the expression levels of MyD88-dependent TLRs in diabetic kidneys. (**A**) Detection of the MyD88-dependent TLR expression levels by Western blot. (**B**) Semiquantitative analysis of the MyD88-dependent TLR expression levels. Protein expression data are presented as means ± SD. *P < 0.05 versus CON.
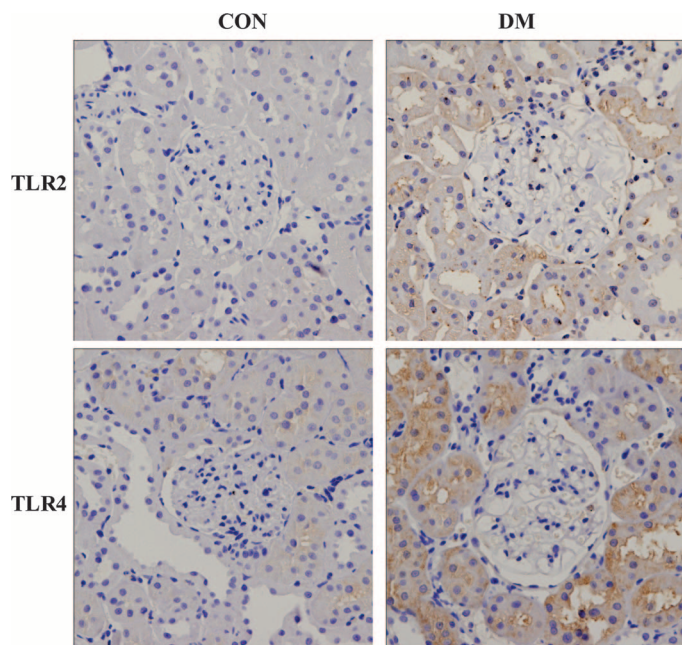

Fig. 4. Immunohistochemical detection of the TLR2 and TLR4 expression levels in diabetic kidneys.

Activation and expression changes of MyD88-dependent signaling pathway molecules in diabetic kidneys

Western blot analysis revealed significant up-regulation of the TLR adaptive molecule MyD88 and activation of the downstream signaling kinase molecule IRAK-1 (the phospho–IRAK-1 level was significantly increased) in DM kidneys compared with CON kidneys (Fig. 5), indicating that the MyD88-dependent pathway was significantly activated in the kidneys of diabetic pigs.

Changes in MyD88-independent TLRs and downstream signaling pathway molecules in diabetic kidneys

We used Western blot analysis to detect the changes in TLR3 and TLR4 expression and the activation of transcription factor IRF-3 (downstream signaling pathway component of TLR3 and TLR4) in the kidney tissues from two groups of miniature pigs. The results showed that the levels of TLR3, TLR4, and activated IRF-3 (phospho–IRF-3) were significantly higher in the DM kidneys than in the CON kidneys (Fig. 6), indicating that in the diabetic kidney tissues, TLR3 and TLR4 could also activate the downstream transcription factor IRF-3 through the MyD88-independent pathway.

Activation of the NF-κB signaling pathway in diabetic kidneys

Activation of the TLR system can further induce activation of the NF-κB signaling pathway and promote production of downstream proinflammatory factors. Therefore, we used Western blot to assess the expression or activation statuses of the NF-κB signaling pathway molecules IKKβ, IκB, and NF-κB. The results showed that in the DM kidneys, the levels of NF-κB signaling pathway molecules phospho-IKKβ (activated IKKβ),
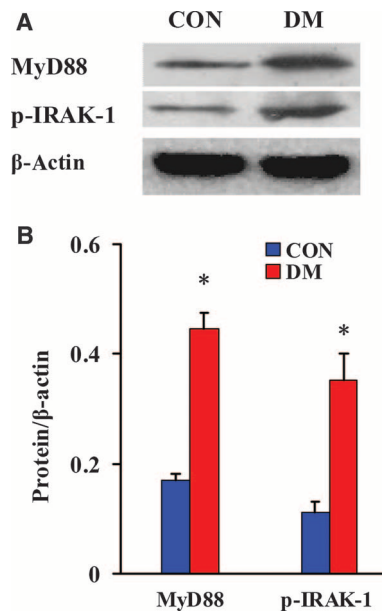

Fig. 5. Western blot analysis of the expression and activation of MyD88-dependent downstream signaling molecules in diabetic kidneys. (**A**) Detection of the expression and activation of MyD88-dependent downstream signaling molecules by Western blot. (**B**) Semiquantitative analysis of the expression and activation levels of MyD88-dependent downstream signaling molecules. Protein expression data are presented as means ± SD. *P < 0.05 versus CON.
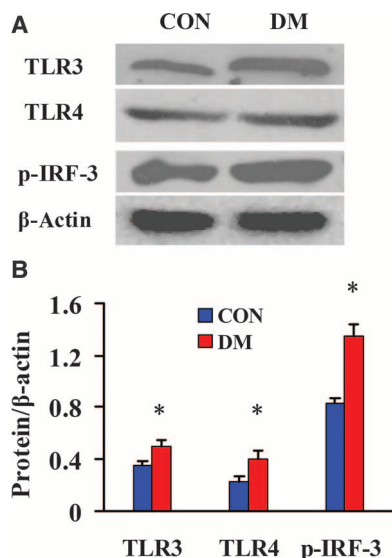
Fig. 6. Western blot analysis of the expression of MyD88-independent TLRs and activation of downstream signaling pathway molecules in diabetic kidneys. (**A**) Detection of the expression of MyD88-independent TLRs and the activation of downstream signaling pathway molecules by Western blot. (**B**) Semiquantitative analysis of the expression of MyD88-independent TLRs and the activation of downstream signaling pathway molecules. Protein expression data are presented as means ± SD. *$P <$ 0.05 versus CON.
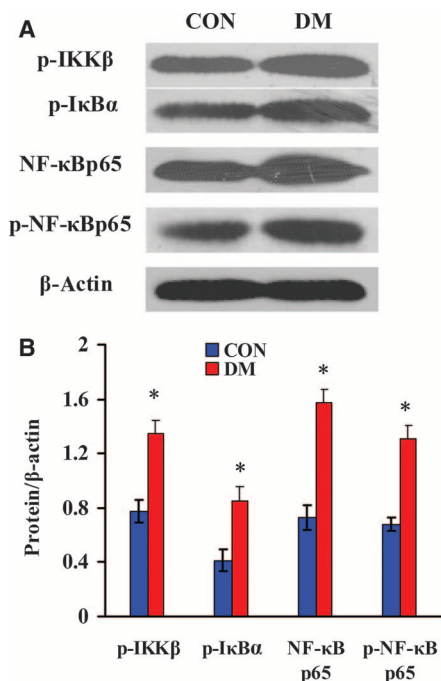

Fig. 7. Western blot analysis of the expression and activation of NF-κB signaling pathway molecules in diabetic kidneys. (**A**) Detection of the expression and activation of NF-κB signaling pathway molecules by Western blot. (**B**) Semiquantitative analysis of the expression and activation of NF-κB signaling pathway molecules. Protein expression data are presented as means ± SD. *$P <$ 0.05 versus CON.

phospho-IκBα (activated IκBα), NF-κBp65, and phospho–NF-κBp65 (activated NF-κBp65) were significantly higher than those in the CON kidneys (Fig. 7), suggesting that the NF-κB signaling pathway was markedly activated during the development of diabetic renal lesions.

Changes in the expression levels of proinflammatory factors in diabetic kidneys

We used quantitative real-time polymerase chain reaction (qRT-PCR) to detect the changes in the mRNA expression levels of proinflammatory factors including cytokines, chemokines, and adhesion molecules IL-6 (interleukin-6), MIP-2, MCP-1, CCL5, and VCAM-1 (vascular cell adhesion molecule–1). The results showed that the expression levels of IL-6, MIP-2, MCP-1, CCL5, and VCAM-1 were significantly
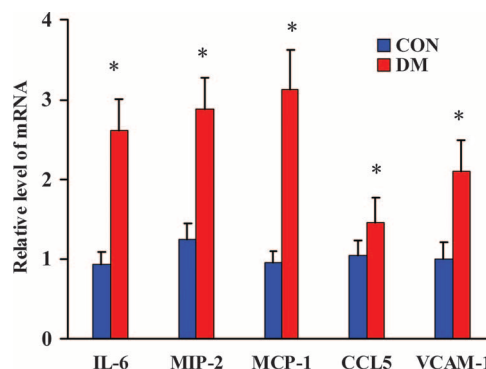

Fig. 8. qRT-PCR detection of the mRNA expression levels of proinflammatory factors in the kidneys from diabetic miniature pigs. *$P <$ 0.05 versus CON.
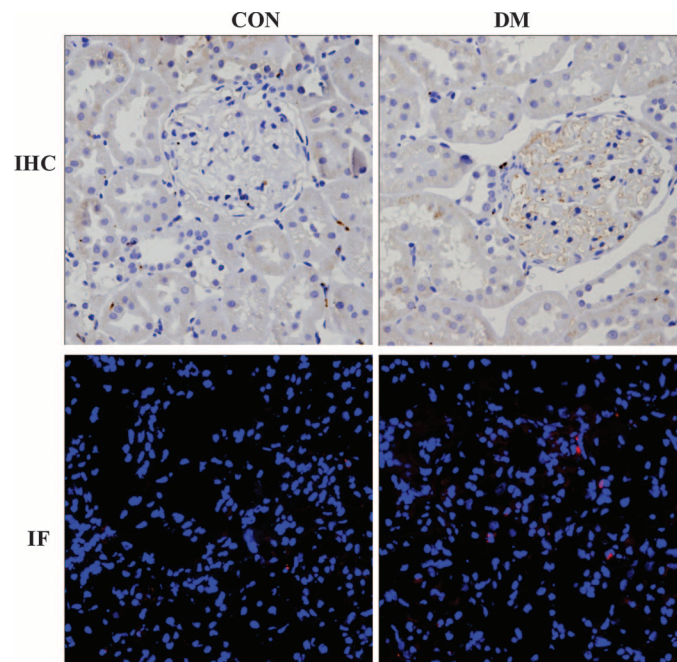

Fig. 9. Immunofluorescent (magnification, ×200) and immunohistochemical (magnification, ×400) detection of CD68 expression in diabetic kidneys. IHC, immunohistochemistry; IF, immunofluorescence.

up-regulated in DM renal tissues (Fig. 8), indicating that inflammation was significantly induced and activated in diabetic renal tissues.

Macrophage infiltration in the kidneys of diabetic miniature pigs

We used immunohistochemistry and immunofluorescence to detect the expression of CD68, a macrophage marker, in renal tissues. The results showed rare CD68-positive macrophage accumulation in CON kidneys. However, there was a significant relative increase in macrophage infiltration in DM kidneys (Fig. 9).

DISCUSSION

TLRs comprise an innate immune system receptor superfamily and can further activate downstream inflammation response signaling pathways such as the NF-κB pathway, and thus initiate and induce acquired immune responses (18, 19). In addition to pathogen-associated molecular patterns, some endogenous molecules associated with cell damage, designated as damage-associated molecular patterns such as nuclear DNA binding protein HMGB1 and HSPs and damaged mitochondrial DNA (20), can induce inflammatory responses through binding to TLRs intracellularly and extracellularly (21). Here, we established an animal model of early-stage human-like type 2 diabetes by feeding a high-fat, high-sugar diet to Guangxi Bama miniature pigs and determined the expression levels of TLR endogenous ligands HSP70 and HMGB1 in kidneys. We found that HSP70 was significantly up-regulated in diabetic kidney tissues. In addition to these endogenous damaged molecules, metabolic substrates such as high glucose and free fatty acids could induce cells to release endogenous ligands (such as HSPs) and promote inflammatory responses in mouse glomerular endothelial cells, podocytes, or mesangial cells (6, 8, 22–25). Therefore, the metabolic substrates associated with diabetes may directly interact with TLRs or indirectly promote the production of endogenous TLR ligands, consequently triggering the downstream inflammatory response signaling pathway and prompting the development of diabetes and diabetic complications.

When activated, TLRs recruit different adapter molecules (for example, MyD88) and subsequently initiate diverse downstream signaling cascades, including MyD88-dependent and MyD88-independent pathways, resulting in the activation of transcription factors NF-κB and IRF-3, respectively, and the production of downstream proinflammatory cytokines. In addition to inflammatory and autoimmune kidney diseases, activation of TLR2 and TLR4 is involved in renal inflammation, leukocyte infiltration, and progressive fibrosis in nonimmune kidney diseases such as ischemia/reperfusion injuries, tubulointerstitial nephritis, and nephrotoxicity (26, 27).

Although TLR2 and TLR4 are up-regulated in diabetic rats, the role of all members of the TLR system in diabetic kidney lesions remains unclear. Moreover, given the considerable generic differences between the human and rodent immune systems, including the cellular TLR expression patterns, DN pathologies, and disease duration, the results obtained in rodents cannot be easily extrapolated to human diseases. Because miniature pigs are more similar to humans, we systematically determined the expression and activation status of MyD88-dependent TLRs (TLR1, TLR2, and TLR4 to TLR11) and their downstream signaling molecules MyD88 and IRAK-1 in the miniature pig diabetic model. We found that the expression of MyD88-dependent

TLR2, TLR4, TLR5, TLR7, TLR8, and TLR11, MyD88, and activated IRAK-1 (phospho–IRAK-1) were significantly up-regulated. We also found that the expression levels of MyD88-independent TLR3 and TLR4 and activated IRF-3 were significantly increased in diabetic kidneys. These findings suggested that in the diabetic kidneys, both MyD88-dependent and MyD88-independent TLRs were significantly up-regulated and could further activate downstream signaling pathway molecules. NF-κB is a key transcription factor that can induce the inflammation response. Studies have shown that excess nutrients can induce tissue inflammation by activating the NF-κB signaling pathway and promoting the expression of inflammatory cytokines (3). TLRs can activate the NF-κB signaling pathway molecules IRAK-1, IKK, IκB, and NF-κBp65 via MyD88 (28–31). Here, we found that the levels of phospho-IKKβ, phospho-IκBα, NF-κBp65, and phospho–NF-κBp65 were significantly increased, indicating that the NF-κB signaling pathway was significantly activated after diabetes-associated kidney damage.

Recent studies have shown that innate immune receptor–mediated signaling pathways play an important role in metabolic inflammation in diabetes (1). This suggests that the intake of excess nutrients and metabolites could induce inflammatory responses. The molecular mechanisms and signaling pathways of metabolic inflammation are similar to those of traditional pathogen-induced inflammation, although metabolic inflammation is chronic and low-level (4, 32). It has been shown that abnormal immune responses induced by excessive nutrient intake represent the primary cause of metabolic inflammation (32). Here, we found that the expression levels of the proinflammatory factors IL-6, MIP-2, MCP-1, CCL and VCAM-1 as well as the macrophage marker CD68 were significantly increased in the diabetes group, indicative of a corresponding increase in the renal expression of inflammatory factors and inflammatory cell (macrophages) infiltration during diabetes.

This study demonstrated that in the kidneys from the diabetic miniature swine model, the expression levels of endogenous TLR ligands and various TLRs were significantly up-regulated and may subsequently activate NF-κB and IRF-3 signaling through MyD88-dependent and MyD88-independent pathways to cause metabolic inflammation in kidney tissues, ultimately leading to the occurrence and development of diabetic renal damage. This study provides a foundation for the future development of inhibitors that target TLR signaling pathway molecules and for their use in the treatment of diabetic renal injuries.

MATERIALS AND METHODS

Experimental animals

A total of 24 male miniature pigs, 4 months of age, were obtained from Bama County, Guangxi, China, and housed in the Institute of Animal Science, Chinese Academy of Agricultural Sciences in Beijing. Chinese Bama mini pigs have been produced by inbreeding of half-siblings, resulting in the animal's characteristic small size, stable genetics, and uniform phenotypes. The housing conditions were as follows: room temperature of 19° to 29°C and humidity of 40 to 70%. Miniature pigs were randomly divided into two groups: the control diet group (CON; n = 10), which was fed a basal diet, and the DM group (DM; n = 14), which was fed a high-sugar and high-fat diet comprising 51% basal diet, 37% sucrose, 2% cholesterol, and 10% lard. The daily feeding amount was 3% weight of mini pigs, which were fed twice

daily. Pigs were weighed weekly, and meal size was adjusted to the weight of the pig. Water was available ad libitum. The total study period was 8 months. All experiments involving animals were approved by the Institutional Animal Care and Use Committee at the Chinese PLA General Hospital.

Blood biochemical assay

During the feeding process, blood samples were collected monthly from the orbital sinuses of pigs that had been fasted overnight to measure fasting GLU, INS, TG, CHOL, HDL-C, LDL-C, creatinine, and BUN. The GLU oxidase method was used to measure serum GLU. TG, CHOL, HDL-C, and LDL-C were determined using the oxidase method. BUN and creatinine were determined using a colorimetric method. Serum insulin was determined using a radioimmunoassay.

Pathological analysis of renal tissues

After 8 months of feeding, the mini pigs were anesthetized and the kidney tissues were excised, fixed in 4% paraformaldehyde, embedded in paraffin, and sectioned at 4 μm. Sections stained with PAS were used to evaluate the pathological changes in renal structure in DM mini pigs. The glomerular area was analyzed using Image-Pro Plus software (Media Cybernetics Inc.) by randomly selecting at least 50 glomeruli. All statistical data were expressed as means ± SD ($x \pm s$).

Western blot

The frozen left kidney tissues were lysed with RIPA (radioimmunoprecipitation assay) lysis buffer [50 mM tris-Cl (pH 7.6), 150 mM NaCl, 1% NP-40, 0.1% SDS, 0.5% deoxycholic acid, leupeptin (1 μg/ml), aprotinin (1 μg/ml), and 0.5 mM phenylmethylsulfonyl fluoride] and were centrifuged at 12,000g at 4°C for 30 min to collect cellular proteins in the supernatants. When the phosphorylated proteins were analyzed, 50 mM sodium fluoride (Ser/Thr phosphatase inhibitor) and 0.2 mM sodium orthovanadate (Tyr phosphatase inhibitor) were added. Equal amounts of proteins from each sample were resolved by 6 to 15% SDS–polyacrylamide gel electrophoresis, transferred to nitrocellulose membranes, blocked with 5% skim milk for 1 hour at room temperature, and probed with the following primary human antigens at 4°C overnight. The detailed information on the primary antibodies used is presented in Table 2. The blots were subsequently incubated with horseradish peroxidase–conjugated anti-mouse or anti-rabbit immunoglobulin G (IgG; Santa Cruz Biotechnology) at 1:1000 to 1:5000. Immunoreactive bands were visualized via enhanced chemiluminescence, and densitometry was performed using Quantity One software (Bio-Rad Laboratories).

Immunohistochemistry analysis

Kidneys were fixed in 10% formaldehyde overnight at 4°C and processed for paraffin embedding according to standard procedures. Sections were

Table 2. Detailed information on the primary antibodies used. NA, unavailable amino acid sequence for pig proteins; Ab, antibody.

Antibody	Company	Catalog no.	Pig homology with human (amino acid sequence)
HMGB1	Novus Biologicals	NB100-2322	99%; this Ab has been verified to react with pig HMGB1
HSP70	Santa Cruz Biotechnology	sc-66048	NA; this Ab has been verified to react with pig HSP70
β-Actin	Cell Signaling Technology	#4967	100%; this Ab has been verified to react with pig β-actin
TLR1	Abnova	PAB0215	89%
TLR2	Abcam	ab108998	87%
TLR3	Abcam	ab53424	91%; this Ab has been predicted to react with pig TLR3
TLR4	Abcam	ab22048	84%
TLR5	Abcam	ab62460	86%
TLR6	Santa Cruz Biotechnology	sc-30001	88%; this Ab has been predicted to react with pig TLR6
TLR7	Abcam	ab113524	92%; this Ab has been predicted to react with pig TLR7
TLR8	Santa Cruz Biotechnology	sc-25467	83%
TLR9	Abcam	ab12121	86%
TLR10	Santa Cruz Biotechnology	sc-30198	89%
TLR11	Abnova	PAB11333	NA
MyD88	Abcam	ab36076	89%; this Ab has been predicted to react with pig MyD88
Phospho–IRAK-1	Santa Cruz Biotechnology	sc-130197	83%
Phospho–IRF-3	Cell Signaling Technology	#4947	83%; this Ab has been verified to react with pig IRF-3
Phospho-IKKβ	Abcam	ab59195	NA
Phospho-IκBα	Cell Signaling Technology	#9246	95%; this Ab has been verified to react with pig IκBα
NF-κBp65	Abcam	ab31481	NA; this Ab has been verified to react with pig NF-κBp65
Phospho–NF-κBp65	Cell Signaling Technology	#3033	NA; this Ab has been verified to react with pig NF-κBp65
CD68	Santa Cruz Biotechnology	sc-9139	NA

cut at 3-μm thickness. For immunohistochemical analyses, some tissue sections were subjected to antigen retrieval by microwaving or autoclaving for 10 or 15 min in 10 mM sodium citrate buffer (pH 6.0). Endogenous peroxidase activity was blocked by a 10-min incubation in 3% hydrogen peroxide. Sections were washed with phosphate-buffered saline (PBS) and subsequently incubated with 1.5% normal goat serum for 20 min, followed by overnight incubation with primary antibodies (1:50 anti-CD68 antibody; 1:200 anti-TLR2 and anti-TLR4 antibodies) at 4°C. After three washes with PBS, the samples were incubated with biotin-conjugated anti-IgG for 30 min at room temperature. After another wash in PBS, the sections were incubated with a streptavidin-conjugated peroxidase (Invitrogen) for 30 min at room temperature. After a final wash in PBS, the sections were incubated with diaminobenzidine (Invitrogen) followed by microscopic examination.

Immunofluorescence analysis

Renal tissues were embedded in OCT compound. Cryostat sections (4 μm) were stained with a 1:500 anti-CD68 antibody dilution. Sections were incubated with a 1:400 Cy3-conjugated anti-IgG dilution. Finally, DAPI (4′,6-diamidino-2-phenylindole) double staining followed by slide mounting was performed. The results were analyzed under an Olympus laser scanning confocal microscope (Olympus Corp.).

qRT-PCR detection of proinflammatory cytokine expression in renal tissues

Total RNA was isolated from renal tissues with TRIzol (Invitrogen) according to the manufacturer's instructions. Reverse transcription was performed with a TIANScript RT kit (Tiangen Biotech). Amplification was performed on a 7500 Real-Time PCR System (Applied Biosystems). The reactions contained 50 ng of complementary DNA, 0.2 μM primer concentrations, and 10 μl of 2× SYBR Green buffer (TaKaRa) in a final volume of 20 μl. The following primers were designed using the software package Primer Express 2.0 (Applied Biosystems) and based on GenBank nucleotide sequences: IL-6 (accession: JQ839263.1): forward, 5′-GGGAAATGTCGAGGCTGTG-3′ and reverse, 5′-AGGGGTGGTGGCTTTGTCT-3′; MIP-2 (accession: NM_001001861.1): forward, 5′-CGGAAGTCATAGCCACTCT-CAA-3′ and reverse, 5′-CAGTAGCCAGTAAGTTTCCTCCATC-3′; MCP-1 (accession: NM_213816.1): forward, 5′-GGGTATTTAGGG-CAAGTTAGAAGGA-3′ and reverse, 5′-CATAAGCCACCTGG-ACAAGAAAA-3′; CCL5 (accession: NM_001129946.1): forward, 5′-GTGTGTGCCAACCCAGAGAA-3′ and reverse, 5′-GGACAAG-AGCAAGAAGCAGTAGG-3′; VCAM-1 (accession: NM_213891.1): forward, 5′-AGCACTTTCAGGGAGGACACA-3′ and reverse, 5′-AACGGCAAACACCATCCAA-3′; and glyceraldehyde-3-phosphate dehydrogenase (accession: NM_001206359.1): forward, 5′-TCCCTG-CTTCTACCGGCGCT-3′ and reverse, 5′-ACACGTTGGGGGTGG-GGACA-3′. PCR was performed with the following cycling conditions: 95°C for 30 s and 40 cycles of denaturation at 95°C for 15 s and extension at 60°C for 30 s. All samples were run in triplicate. The relative target mRNA abundances were determined according to the comparative cycle threshold method.

Statistical analysis

Statistical analysis was performed using the SPSS 17.0 statistical software package, and all statistical data were presented as $x \pm$ SD. A value of $P < 0.05$ was considered to indicate statistical significance.

REFERENCES AND NOTES

1. R. G. Baker, M. S. Hayden, S. Ghosh, NF-κB, inflammation, and metabolic disease. *Cell Metab.* **13**, 11–22 (2011).
2. M. Kitada, A. Takeda, T. Nagai, H. Ito, K. Kanasaki, D. Koya, Dietary restriction ameliorates diabetic nephropathy through anti-inflammatory effects and regulation of the autophagy via restoration of Sirt1 in diabetic Wistar fatty (*fa/fa*) rats: A model of type 2 diabetes. *Exp. Diabetes Res.* **2011**, 908185 (2011).
3. D. Cai, T. Liu, Inflammatory cause of metabolic syndrome via brain stress and NF-κB. *Aging* **4**, 98–115 (2012).
4. G. S. Hotamisligil, Inflammation and metabolic disorders. *Nature* **444**, 860–867 (2006).
5. R. Yang, J. M. Trevillyan, c-Jun N-terminal kinase pathways in diabetes. *Int. J. Biochem. Cell Biol.* **40**, 2702–2706 (2008).
6. H. Kaur, A. Chien, I. Jialal, Hyperglycemia induces Toll like receptor 4 expression and activity in mouse mesangial cells: Relevance to diabetic nephropathy. *Am. J. Physiol. Renal Physiol.* **303**, F1145–F1150 (2012).
7. S. Devaraj, P. Tobias, B. S. Kasinath, R. Ramsamooj, A. Afify, I. Jialal, Knockout of Toll-like receptor-2 attenuates both the proinflammatory state of diabetes and incipient diabetic nephropathy. *Arterioscler Thromb. Vasc. Biol.* **31**, 1796–1804 (2011).
8. F. Li, N. Yang, L. Zhang, H. Tan, B. Huang, Y. Liang, M. Chen, X. Yu, Increased expression of Toll-like receptor 2 in rat diabetic nephropathy. *Am. J. Nephrol.* **32**, 179–186 (2010).
9. M. Lin, W. H. Yiu, R. X. Li, H. J. Wu, D. W. Wong, L. Y. Chan, J. C. Leung, K. N. Lai, S. C. Tang, The TLR4 antagonist CRX-526 protects against advanced diabetic nephropathy. *Kidney Int.* **83**, 887–900 (2013).
10. J. Satriano, H. Mansoury, A. Deng, K. Sharma, V. Vallon, R. C. Blantz, S. C. Thomson, Transition of kidney tubule cells to a senescent phenotype in early experimental diabetes. *Am. J. Physiol. Cell Physiol.* **299**, C374–C380 (2010).
11. J. Seok, H. S. Warren, A. G. Cuenca, M. N. Mindrinos, H. V. Baker, W. Xu, D. R. Richards, G. P. McDonald-Smith, H. Gao, L. Hennessy, C. C. Finnerty, C. M. López, S. Honari, E. E. Moore, J. P. Minei, J. Cuschieri, P. E. Bankey, J. L. Johnson, J. Sperry, A. B. Nathen, T. R. Billiar, M. A. West, M. G. Jeschke, M. B. Klein, R. L. Gamelli, N. S. Gibran, B. H. Brownstein, C. Miller-Graziano, S. E. Calvano, P. H. Mason, J. P. Cobb, L. G. Rahme, S. F. Lowry, R. V. Maier, L. L. Moldawer, D. N. Herndon, R. W. Davis, W. Xiao, R. G. Tompkins; the Inflammation and Host Response to Injury, Large Scale Collaborative Research Program, Genomic responses in mouse models poorly mimic human inflammatory diseases. *Proc. Natl. Acad. Sci. U.S.A.* **110**, 3507–3512 (2013).
12. M. A. Groenen, A. L. Archibald, H. Uenishi, C. K. Tuggle, Y. Takeuchi, M. F. Rothschild, C. Rogel-Gaillard, C. Park, D. Milan, H.-J. Megens, S. Li, D. M. Larkin, H. Kim, L. A. F. Frantz, M. Caccamo, H. Ahn, B. L. Aken, A. Anselmo, C. Anthon, L. Auvil, B. Badaoui, C. W. Beattie, C. Bendixen, D. Berman, F. Blecha, Analyses of pig genomes provide insight into porcine demography and evolution. *Nature* **491**, 393–398 (2012).
13. M. M. Swindle, A. Makin, A. J. Herron, F. J. Clubb Jr., K. S. Frazier, Swine as models in biomedical research and toxicology testing. *Vet. Pathol.* **49**, 344–356 (2012).
14. S. Giraud, F. Favreau, N. Chatauret, R. Thuillier, S. Maiga, T. Hauet, Contribution of large pig for renal ischemia-reperfusion and transplantation studies: The preclinical model. *J. Biomed. Biotechnol.* **2011**, 532127 (2011).
15. M. N. Simmons, M. J. Schreiber, I. S. Gill, Surgical renal ischemia: A contemporary overview. *J. Urol.* **180**, 19–30 (2008).
16. G. Bode, P. Clausing, F. Gervais, J. Loegsted, J. Luft, V. Nogues, J. Sims; Steering Group of the RETHINK Project, The utility of the minipig as an animal model in regulatory toxicology. *J. Pharmacol. Toxicol. Methods* **62**, 196–220 (2010).
17. Y. Zhang, Y. Shi, Y. Liu, H. Dong, M. Liu, Y. Li, H. Duan, Growth pattern switch of renal cells and expression of cell cycle related proteins at the early stage of diabetic nephropathy. *Biochem. Biophys. Res. Commun.* **363**, 159–164 (2007).
18. H. J. Anders, D. Schlöndorff, Toll-like receptors: Emerging concepts in kidney disease. *Curr. Opin. Hypertens.* **16**, 177–183 (2007).
19. M. Nishimura, S. Naito, Tissue-specific mRNA expression profiles of human toll-like receptors and related genes. *Biol. Pharm. Bull.* **28**, 886–892 (2005).
20. T. Oka, S. Hikoso, O. Yamaguchi, M. Taneike, T. Takeda, T. Tamai, J. Oyabu, T. Murakawa, H. Nakayama, K. Nishida, S. Akira, A. Yamamoto, I. Komuro, K. Otsu, Mitochondrial DNA that escapes from autophagy causes inflammation and heart failure. *Nature* **485**, 251–255 (2012).
21. M. Lin, S. C. Tang, Toll-like receptors: Sensing and reacting to diabetic injury in the kidney. *Nephrol. Dial. Transplant.* **29**, 746–754 (2014).
22. G. Wolf, J. Bohlender, T. Bondeva, T. Roger, F. Thaiss, U. O. Wenzel, Angiotensin II upregulates Toll-like receptor 4 on mesangial cells. *J. Am. Soc. Nephrol.* **17**, 1585–1593 (2006).
23. J. F. Navarro-González, C. Mora-Fernández, M. Muros de Fuentes, J. García-Pérez, Inflammatory molecules and pathways in the pathogenesis of diabetic nephropathy. *Nat. Rev. Nephrol.* **7**, 327–340 (2011).
24. S. Takata, Y. Sawa, T. Uchiyama, H. Ishikawa, Expression of Toll-like receptor 4 in glomerular endothelial cells under diabetic conditions. *Acta Histochem. Cytochem.* **46**, 35–42 (2013).

25. M. Lin, W. H. Yiu, H. J. Wu, L. Y. Chan, J. C. Leung, W. S. Au, K. W. Chan, K. N. Lai, S. C. Tang, Toll-like receptor 4 promotes tubular inflammation in diabetic nephropathy. *J. Am. Soc. Nephrol.* **23**, 86–102 (2012).

26. H. Wu, G. Chen, K. R. Wyburn, J. Yin, P. Bertolino, J. M. Eris, S. I. Alexander, A. F. Sharland, S. J. Chadban, TLR4 activation mediates kidney ischemia/reperfusion injury. *J. Clin. Invest.* **117**, 2847–2859 (2007).

27. B. Zhang, G. Ramesh, S. Uematsu, S. Akira, W. B. Reeves, TLR4 signaling mediates inflammation and tissue injury in nephrotoxicity. *J. Am. Soc. Nephrol.* **19**, 923–932 (2008).

28. S. Akira, K. Takeda, Toll-like receptor signalling. *Nat. Rev. Immunol.* **4**, 499–511 (2004).

29. F. Y. Liew, D. Xu, E. K. Brint, L. A. O'Neill, Negative regulation of Toll-like receptor-mediated immune responses. *Nat. Rev. Immunol.* **5**, 446–458 (2005).

30. T. Eleftheriadis, B. R. Lawson, Toll-like receptors and kidney diseases. *Inflamm. Allergy Drug Targets* **8**, 191–201 (2009).

31. A. Rivero, C. Mora, M. Muros, J. García, H. Herrera, J. F. Navarro-González, Pathogenic perspectives for the role of inflammation in diabetic nephropathy. *Clin. Sci.* **116**, 479–492 (2009).

32. M. I. Schmidt, B. B. Duncan, Diabesity: An inflammatory metabolic condition. *Clin. Chem. Lab. Med.* **41**, 1120–1130 (2003).

Citation: Y. Feng, S. Yang, Y. Ma, X.-Y. Bai, X. Chen, Role of Toll-like receptors in diabetic renal lesions in a miniature pig model. *Sci. Adv.* **1**, e1400183 (2015).